Environ. Sci. Technol. **2008,** *42,* 2937–2942

Emission Factor for Antimony in Brake Abrasion Dusts as One of the Major Atmospheric Antimony Sources

AKIHIRO IIJIMA,*,†,‡ KEIICHI SATO,‡ KIYOKO YANO,§ MASAHIKO KATO,† KUNIHISA KOZAWA,† AND NAOKI FURUTA‡

Gunma Prefectural Institute of Public Health and Environmental Sciences, 378 Kamioki, Maebashi, Gunma 371-0052, Japan, Department of Applied Chemistry, Faculty of Science and Engineering, Chuo University, 1-13-27 Kasuga, Bunkyo-ku, Tokyo 112-8551, Japan, and Akebono Brake Industry, Co., Ltd., 5-4-71 Higashi, Hanyu, Saitama 348-8509, Japan

Received August 28, 2007. Revised manuscript received November 21, 2007. Accepted December 22, 2007.

Abrasion tests were conducted using a brake dynamometer to determine the antimony (Sb) emission factor originating from automobiles. Abrasion dusts from commercially available brake pads (nonasbestos organic type) were emitted into an enclosed chamber under various braking conditions in terms of initial driving speed and deceleration. Suspended dusts inside the chamber were collected on a quartz fiber filter and weighed. From the experimental data, dust emission could be regressed as a function of the initial kinetic energy loading and the braking time. Using the regression function, the emission factors of brake abrasion dusts under the typical braking conditions (initial driving speed; 50 km/h, deceleration; 1.0 m/s^2) were calculated as 5.8 mg/braking/car for PM_{10} and 3.9 mg/braking/car for $PM_{2.5}$. The elemental composition of the collected dusts indicated that the fraction originating from disk wear contributed to approximately 30% of the suspended dusts. From these analytical results, it was concluded that the Sb emission factors originating from automobiles were approximately 32 μg Sb/braking/car for PM_{10} and 22 μg Sb/braking/car for $PM_{2.5}$. These essential data will contribute to the modeling of atmospheric Sb concentration alongside roadways and also to the better understanding of Sb source apportionment.

Introduction

The relationship between $PM_{2.5}$ concentration and adverse effects for human health has been extensively demonstrated by a large number of epidemiological studies (*1–5*). During the past decade, attention has been focused on the various kinds of harmful chemicals contained in fine airborne particles from both an environmental and toxicological viewpoint. Recently, enrichment of antimony (Sb), one of the harmful elements (*6, 7*), in airborne particles was observed in several countries including Germany (*8*), the U.S. (*9*), Japan (*10*), and Argentina (*11*). Moreover, the Sb enrichment factor has increased even in Arctic ice as much as 50% during the last three decades (*12*). From the various viewpoints of source evaluations using elemental compositions, particle size, and shape distributions, automotive brake abrasion dusts were suspected as one of the important sources of Sb-enriched airborne particles (*8, 10–16*). It is, therefore, essential to determine the Sb emission factor that originates from automotive braking in order to quantitatively evaluate the contribution of automobiles to the atmospheric Sb concentration. The emission factors of pollutants from automobiles have been officially assessed in projects such as MOBILE6 established by the U.S. Environmental Protection Agency (*17*) and JCAP (Japan Clean Air Program) established by JPEC (Japan Petroleum Energy Center) (*18*). In the MOBILE6 project, the emission factor of brake abrasion dusts originating from asbestos brake pads was determined as 13 mg/mi for PM_{10}. However, use of the mileage-based emission factor is not really practical because the emission of the brake abrasion dusts occurs only during braking, whereas exhaust gas is continuously emitted. Instead perhaps, atmospheric Sb distributes specifically depending on traffic density, traffic signal patterns, driving speed, and braking force. Moreover, asbestos brake pads have now generally been replaced by low-metallic, semimetallic, or nonasbestos organic (NAO) type pads. In terms of the JCAP project, while the gaseous pollutants from exhaust have been fully evaluated, the emission factor of brake abrasion dusts has not been determined thus far, and the project pointed out that the contribution of brake abrasion dusts to roadside airborne particles should be assessed in detail.

To this end, in this study abrasion tests to determine the dust emission were carried out using a brake dynamometer for NAO type brake pads which are widely installed in Japanese passenger cars. Dust emission (mg/braking/wheel) from automotive braking was obtained as a regression function of certain braking parameters. Moreover, using the regression function the dust emission factor in the course of individual vehicle braking (mg/braking/car) was determined in various cases in terms of vehicle weight and braking condition. Furthermore, the Sb emission factor (μg Sb/braking/car) was calculated from the determined dust emission factor and the elemental analysis of abrasion dusts.

Experimental Method

Experimental Setup. A brake assembly consisting of a cast iron disk and a caliper mounted on a pair of pads was installed in an enclosed chamber ($W \times D \times H = 2$ m $\times$ 1 m $\times$ 1.5 m) constructed of antistatic-finished polyvinyl chloride sheets (see Figure 1). A high-volume air sampler (model 120V, Kimoto Electric Co., Ltd., Japan) was placed near the chamber wall. The top of the sampler was set level with the center of the brake assembly, and the exhaust air was released from the chamber through a ventilation duct. Fresh air was introduced through a quartz fiber filter (2500 QAT-UP, 180 $\times$ 230 mm, Pallflex Products Co., U.S.) located at the opposite side of the high-volume air sampler. In order to continuously monitor size-classified particle number concentrations of brake abrasion dusts, the sample intake of the aerodynamic particle sizer (APS) spectrometer (model 3321 APS, Tokyo Dylec Co., Japan) (*19, 20*) was placed just 300 mm below the pads.

Operating Conditions of the Brake Dynamometer and Sample Collection. Three types of commercially available NAO pads (referred to as I, II, and III; the same pads labeled

* Corresponding author phone: +81-27-232-4881; fax: +81-27-234-8438; e-mail: iijima-akihiro@pref.gunma.jp.
† Gunma Prefectural Institute of Public Health and Environmental Sciences.
‡ Chuo University.
§ Akebono Brake Industry, Co., Ltd.

10.1021/es702137g CCC: $40.75
Published on Web 03/12/2008

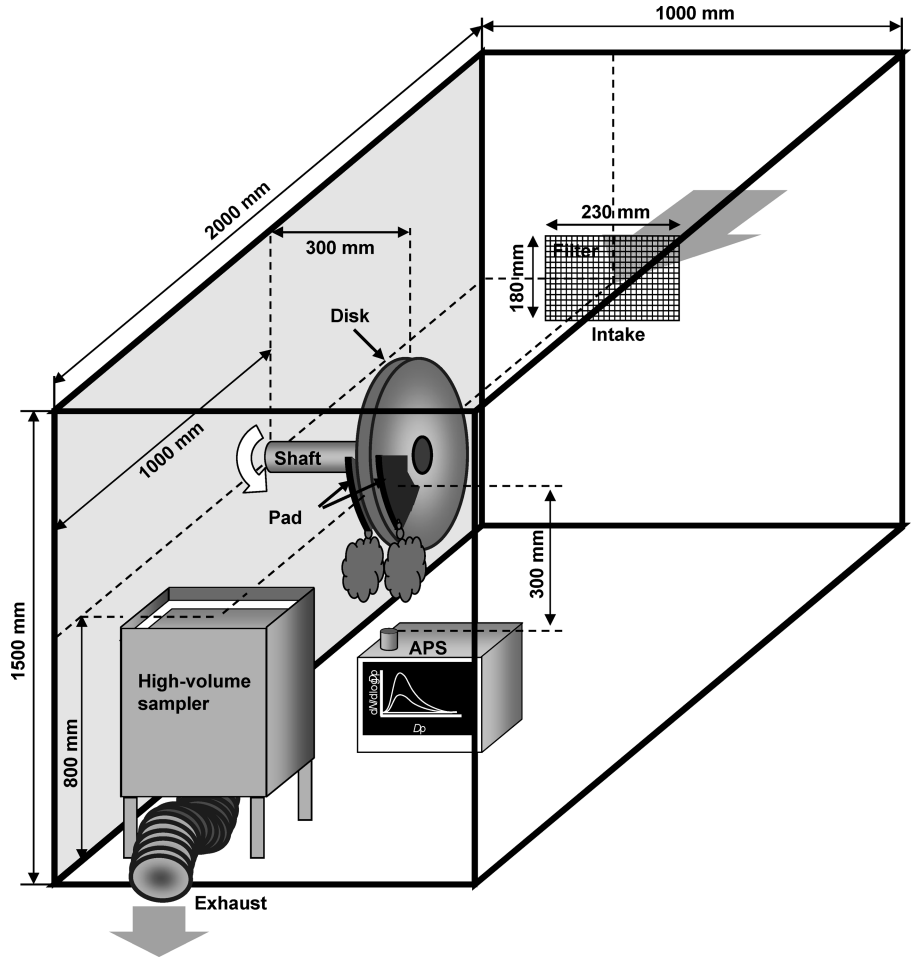

FIGURE 1. Layout of a full-size brake dynamometer assembly and measurement instruments.

B, A, and C, respectively, used in our previous study (*16*)) were used for the abrasion tests. These three pads are provided by three major Japanese brake manufacturers, and they are well distributed to Japanese passenger cars. The market share of these three manufacturers covers approximately 75% of the total Japanese market. Before the abrasion tests, the friction surface was sufficiently burnished to remove roughness.

First, abrasion tests (runs no. 1–9) for pad I were carried out by changing the number of brakings, initial driving speed (40–60 km/h), and deceleration (1.0–3.0 m/s^2) as shown in Table 1. All experimental conditions simulated front wheel braking (braking force distribution (BD); 0.8) of a passenger car (gross vehicle weight (*W*); 2000 kg). The disk and pad temperatures were monitored using a thermocouple attached at 1 mm depth from the friction surface. In order to simulate low-temperature braking in typical urban districts, initial disk temperature was maintained below 100 °C during all runs by taking an interval between brakings. Dust sampling using the high-volume air sampler (flow rate; 1000 L/min) was started just before starting the abrasion tests. The abrasion dusts were collected on a quartz fiber filter (2500 QAT-UP, 180 × 230 mm, Pallflex Products Co.), and the filter was replaced each run. Before and after sampling, the filters were weighed in a temperature and humidity controlled room (temperature 21.5 °C, relative humidity 50%). Particle size distributions of the abrasion dusts were continuously measured by the APS spectrometer with a temporal resolution of 1 s and a size resolution of 52 classes in the range of aerodynamic particle diameter (Dp) = 0.5–20 μm. After the braking operation in each run, in order to collect all abrasion dusts, dust sampling using the high-volume air sampler continued until the APS signals returned to the background level.

TABLE 1. Experimental Conditions for Respective Abrasion Tests

run no.	pad	number of brakings (times)	initial driving speed (km/h)	deceleration (m/s^2)
1	I	15	60	3.0
2	I	15	60	2.0
3	I	15	60	1.0
4	I	20	50	3.0
5	I	20	50	2.0
6	I	20	50	1.0
7	I	30	40	3.0
8	I	30	40	2.0
9	I	30	40	1.0
10	II	15	60	2.0
11	II	20	50	2.0
12	II	30	40	2.0
13	III	15	60	2.0
14	III	20	50	2.0
15	III	30	40	2.0

Next, in order to evaluate the variation in dust emission among the different varieties of pads, the abrasion tests for pads II and III were carried out according to the experimental conditions shown in Table 1. The sampling of abrasion dusts, the weighing of filters, and the measurement of particle size distribution for pads II and III were identical to those for pad I.

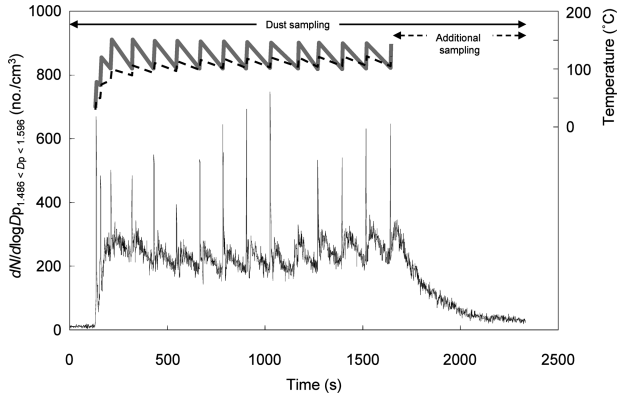

FIGURE 2. Time profiles of the number concentration of abrasion dust particles between *D*p values of 1.486 and 1.596 μm and the disk and pad temperatures obtained during run no. 2 for pad I. Y-axis on the left: thin line (—) indicates the number concentration (no./cm^3) of particles. Y-axis on the right: bold line (—) and broken line (----) indicate the disk temperature and the pad temperature, respectively.

Chemical Analysis of Metallic Elements in Brake Abrasion Dusts. A portion of the sample loaded filter (47 mmφ) was cut out after weighing and subsequently digested by a mixture of 2 mL of hydrofluoric acid (50% atomic absorption spectrometry grade, Kanto Chemical Co., Inc., Japan), 4 mL of nitric acid (60% electronic laboratory grade, Kanto Chemical Co., Inc.) and 1 mL of hydrogen peroxide (30% atomic absorption spectrometry grade, Kanto Chemical Co., Inc.) in a microwave digestion system (Multiwave, Anton Paar GmbH, Austria) under the condition of 700 W for 10 min and 1000 W for further 10 min. Hydrofluoric acid was evaporated by heating the sample solution at 200 °C on a hot plate, and 0.1 mol/L of nitric acid (prepared from 60% nitric acid) was then added to obtain a 50 mL sample. K, Ti, and Fe were determined by an inductively coupled plasma atomic emission spectrometer (ICP-AES, Ciros CCD, Rigaku, Japan), and Cu, Zn, Sb, and Ba were determined by an inductively coupled plasma mass spectrometer (ICP-MS, SPQ9000, Seiko Instrument Inc., Japan). Elemental analysis was conducted under the same conditions as reported previously (*16*). All analytical procedures were validated by the standard reference material SRM 1648 (urban particulate matter) prepared by the NIST (National Institute of Standards and Technology). The analytical results were in good agreement with the certified and reference values.

Results and Discussion

Temporal Profiles of the Number Concentrations and the Particle Size Distributions of Abrasion Dusts. Figure 2 shows the temporal profiles of the disk and the pad temperatures and the number concentration $dN/d\log D$p (no./cm^3) of the abrasion particles between Dp values of 1.486 and 1.596 μm obtained during run no. 2. The initial disk temperature for this individual braking was precisely controlled below 100 °C. For each braking, spike-shaped peaks (possibly due to collision and friction between the disk and the pads) and subsequent increments (possibly due to detachment of the abrasion dusts sticking to the disk or the pad surface) were found. These findings are very similar to our previous observations determined with an open system (*16*). Additional sampling after the braking operation revealed that APS signals (no./cm^3) returned to the background level, indicating that the abrasion dusts were almost completely collected on the filter. The total weight of suspended dusts collected on the filter accounted for 63% of the total wear weight of pad I, with the remaining 37% suspected to have deposited on the chamber bottom as large particles.

APS signals observed during the individual run were normalized by the maximum value in order to eliminate signal variations due to differences in the number of brakings and the total experiment time. The particle size distributions based on the number concentrations for pads I, II, and III are given in Figure 3a, b, and c, respectively. As shown in Figure 3a, the peaks of the number-based distributions were found around 0.8 μm for runs no. 1–9, and these were independent of initial driving speed and deceleration. Moreover, it can be seen in Figure 3a, b, and c that there were no significant differences in the peaks of distribution among the three kinds of pads. We previously reported that the peak of the particle size distribution shifted to the fine side with decreasing disk temperature (400 °C; ≈2 μm, 300 °C; ≈1.5 μm, 200 °C; ≈1 μm) (*16*), and the present observations (100 °C; ≈0.8 μm) are consistent with that tendency. Hence, quite a number of fine particles could be emitted to the atmosphere by low-temperature braking in urban districts.

Under the assumption that the abrasion particles are spherical shape, particle number distributions were converted to the mass distributions by multiplying particle number, volume, and density (Density does not affect the normalized distributions.) (see Figure 3d, e, and f). The mass fractions of PM_{10} accounted for 95–98% (pad I), 97–98% (pad II), and 97–98% (pad III), respectively. On the other hand, those of $PM_{2.5}$ accounted for 59–70% (pad I), 62–69% (pad II), and 56–66% (pad III) of total mass, respectively. Therefore, the emission weight of fine (<2.5 μm) particles were more significant than that of coarse (2.5–10 μm) particles.

Dust Emissions of Various Braking Conditions. Dust emission data (mg/braking/wheel) shown in Table 2 was obtained by dividing the collected dust weight by the applied number of brakings in the individual run. Under the condition of the same deceleration (e.g., run nos. 2, 5, and 8), dust emission increased along with increased initial driving speed. On the other hand, dust emission increased along with decreased deceleration under the condition of the same initial driving speed (e.g., run nos. 4, 5, and 6). Prolonged friction during low deceleration braking might induce fatigue of the pad friction surface. According to the comparison of dust emissions under the same braking condition for the different varieties of pads (run nos. 2, 10, and 13, run nos. 5, 11, and 14, and run nos. 8, 12, and 15), variation was determined as up to 43% (run nos. 8, 12, and 15) as a relative standard deviation.

Dust emissions under certain specific braking conditions have also been reported by Garg et al. (*21*) and Sanders et al. (*22*). Garg et al. (*21*) examined three kinds of semimetallic and four kinds of NAO type brake pads under several disk temperature conditions using an enclosed chamber and reported dust emissions of 0.29–1.66 mg/braking/wheel (semimetallic) and 0.11–0.84 mg/braking/wheel (NAO) under conditions of 50 km/h initial driving speed, 3 m/s^2 deceleration, and 100 °C disk temperature. On the other hand, Sanders et al. (*22*) examined one kind each of low-metallic, semimetallic, and NAO type brake pads using a dilution tunnel and reported dust emissions of 7.0 mg/braking/wheel (low-metallic), 1.7 mg/braking/wheel (semimetallic), and 1.5 mg/braking/wheel (NAO) under the conditions of 90 km/h initial driving speed, <1.6 m/s^2 deceleration, and <160 °C disk temperature. Even though the same NAO type pads are used in passenger vehicles, it is interesting to note that the dust emission data shows a large variation. As previously mentioned, the dust emissions reported here varied depending on the several braking conditions employed, including initial driving speed and deceleration (see Table 2). Moreover, a maximum of 43% variation was observed for the dust emissions among the different pads I, II, and III. Since the

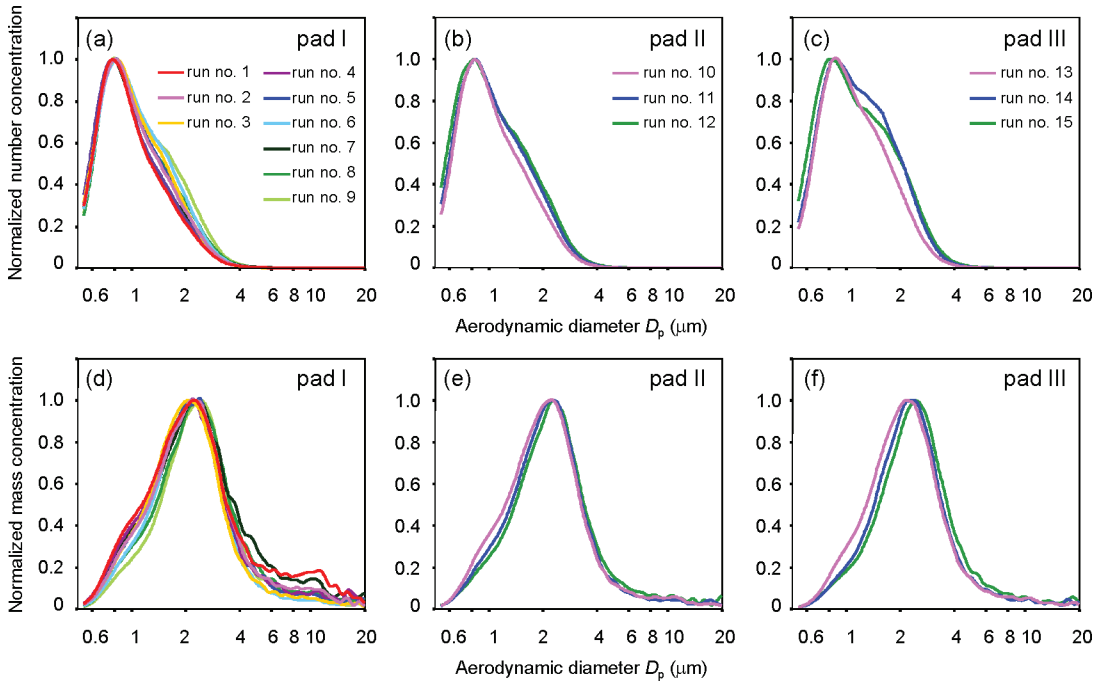

FIGURE 3. Normalized particle size distributions of brake abrasion dusts. a, b, and c show the normalized number distributions for pads I, II, and III, respectively. d, e, and f show the normalized mass distributions converted from a, b, and c. APS signals are normalized by the maximum values.

TABLE 2. Dust Emissions for Various Initial Driving Speeds and Decelerations

		dust emission (mg/braking/wheel) (run no.)					
		initial driving speed (km/h)					
pad	deceleration (m/s^2)	60		50		40	
I	3.0	2.14	(1)	0.91	(4)	0.37	(7)
I	2.0	2.58	(2)	1.15	(5)	0.70	(8)
I	1.0	3.05	(3)	2.06	(6)	1.26	(9)
II	2.0	2.60	(10)	2.21	(11)	1.28	(12)
III	2.0	1.77	(13)	1.39	(14)	0.59	(15)

respective bulk pad compositions are designed to control several braking characteristics such as braking force, wear resistance, and thermal capacity, there is large diversity among the commonly used NAO pads. Therefore, the variations of dust emissions might be mainly caused by the difference of braking conditions and the varieties of pads. In order to determine the emission factor of the brake abrasion dusts, these two main causes should be carefully assessed.

Approximation of Dust Emission by the Automotive Braking Parameters. It became clear that dust emission is dependent on initial driving speed and deceleration. In order to clarify the influencing factor on dust emission, the relationship between dust emission, initial driving speed, and deceleration was systematically evaluated for pad I through run nos. 1–9. Talib et al. (*23*) demonstrated that pad wear was influenced by applied loading to the friction surface and braking time. On the basis of this observation, the relationship between the dust emission (z; mg/braking/wheel), the initial kinetic energy loading to the friction surface (x; Nm/cm^2/wheel) and the braking time (y; sec) obtained in run nos. 1–9 are described in Figure 4. The initial kinetic energy loading to the friction surface was calculated from the gross vehicle weight (W; kg), the initial driving speed (V_0; m/s), the braking force distribution (BD; 0.8 for a pair of the front wheels) and the friction area of a pair of pads (A; cm^2) and expressed as the following eq 1.

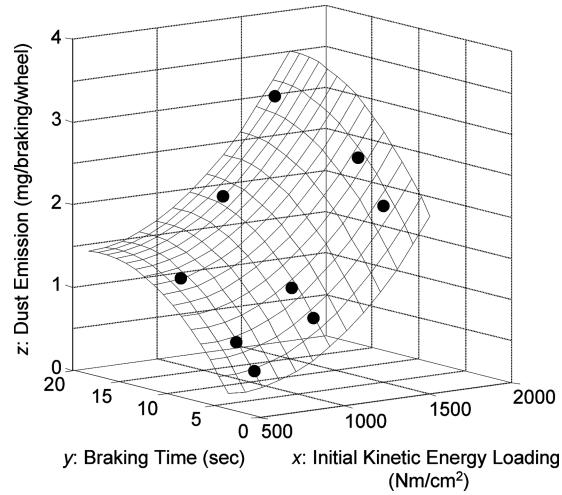

FIGURE 4. Dust emission as a function of initial kinetic energy loading to the friction surface and the braking time. Fitted surface was regressed by the nine experimental data sets (●) obtained in run nos. 1–9 for pad I.

$$x = (1/2) \times W \times V_0 \times (\mathrm{BD}/2) \times (1/A) \quad (1)$$

As shown in Figure 4, the dust emission could be fitted with the initial kinetic energy loading and the braking time, and the regression function could be expressed as the following eq 2 by the least-squares approximation (R^2 = 0.993).

$$z = 1.39 \times 10^{-6}x^2 - 7.19 \times 10^{-3}y^2 + 1.59 \times 10^{-5}xy - 1.61 \times 10^{-3}x + 2.29 \times 10^{-1}\mathrm{y} \quad (2)$$

Equation 2 allowed regression of the dust emission data under the various braking conditions. Nevertheless, extrapolation for data far outside the fitted surface in Figure 4 is not recommended because the wear characteristics might change

TABLE 3. Elemental Concentrations in Abrasion Dusts Originating from Pads and Bulk Pads

	concentration (%)							
	pad I		pad II		pad III		average of three pads	
element	dusts[a]	bulk Pad[b]	dusts[a]	bulk Pad[b]	dusts[a]	bulk pad[b]	mean[c]	%RSD
K	1.4	1.4	3.9	4.1	2.3	1.8	2.6	49
Ti	5.6	4.6	11	9.5	11	8.2	9.4	34
Fe	0.13	0.12	8.6	8.6	0.44	0.36	3.1	157
Cu	13	13	9.9	15	21	18	15	38
Zn	0.11	0.070	0.063	0.031	2.9	3.2	1.0	158
Sb	0.78	0.71	1.7	1.7	1.9	1.6	1.5	41
Ba	14	13	8.1	7.3	14	13	12	29

[a] Values corrected by the disk contribution to the total abrasion dusts. [b] Cited from Iijima et al. (*16*). [c] Values are averaged concentrations of dusts emitted from three different pads.

TABLE 4. Estimation of Emission Factors for Brake Abrasion Dusts and Sb

(a) braking parameters for the estimation

				friction area		
case	gross vehicle weight (kg)	initial driving speed (km/h)	deceleration (m/s^2)	front (cm^2/wheel)	rear (cm^2/wheel)	braking force distribution (front/rear)
1	2500	50	1.0	120	56	0.7/0.3
2	2000	50	1.0	100	56	0.7/0.3
3	1500	50	1.0	80	56	0.7/0.3

(b) estimated emission factors

	dust emission[a] (mg/braking/wheel)		emission factor of abrasion dusts (mg/braking/car)			Sb emission factor (μg Sb/braking/car)		
case	front	rear	total	PM_{10}	$PM_{2.5}$	total	PM_{10}	$PM_{2.5}$
1	1.6	1.5	6.1	5.9	4.0	34	33	22
2	1.5	1.5	5.9	5.7	3.8	33	32	22
3	1.5	1.5	5.9	5.7	3.8	33	32	22
average	1.5	1.5	6.0	5.8	3.9	34	32	22

[a] approximated by eq 2.

drastically due to the overheating of the friction surface. Phenolic resin, the main compound binding the brake components (e.g., Sb_2S_3, $BaSO_4$, Cu fiber, aramid fiber, and $K_2O \cdot nTiO_2$) together, will melt or evaporate at a friction surface temperature above its melting or boiling point. As a result, this may lead to overwearing of pads. However, the dust emission data regressed using eq 2 does cover the typical braking conditions of urban districts.

Mass Fractions of Abrasion Dusts Originating from the Disk or Pad. Brake abrasion dusts contain particles originating from both the disk and the pad. In order to evaluate the exact Sb emission of brake abrasion dusts, the total abrasion dusts must be separated into disk and pad wear. In this estimation, the cast iron disk was assumed to be made from 100% Fe and was used an indicator of disk wear. The dust weight originating from disk wear (W_{disk}) and pad wear (W_{pad}) can be distinguished from the total abrasion dust weight (W_{dusts}) by solving the following simultaneous eqs 3 and 4 which express dust and Fe mass balance.

$$W_{\text{disk}} + W_{\text{pad}} = W_{\text{dusts}} \quad (3)$$

$$[\text{Fe}]_{\text{disk}} \times W_{\text{disk}} + [\text{Fe}]_{\text{pad}} \times W_{\text{pad}} = [\text{Fe}]_{\text{dusts}} \times W_{\text{dusts}} \quad (4)$$

W_{dusts} was obtained by weighing the individual filter sample. In eq 4, $[\text{Fe}]_{\text{disk}}$ (Fe mass concentration (%) in the disk) was fixed as 100%. $[\text{Fe}]_{\text{pad}}$ (Fe mass concentration (%) in the pad) was used as 0.12, 8.6, and 0.36%, for pads I, II, and III, respectively, which were determined in our previous study (*16*). From the elemental analysis of collected abrasion dusts, $[\text{Fe}]_{\text{dusts}}$ was determined in the range of 22–31%, 32–35% and 29–40% for pads I, II, and III, respectively. Consequently, the mass fraction of abrasion dusts originating from the disk ($F_{\text{disk}} = W_{\text{disk}}/W_{\text{dusts}}$) (%) can be estimated to be 28, 27, and 34% as an averaged value for pads I, II, and III, respectively.

The elemental concentrations in the abrasion dusts originating from the pad which were corrected to exclude the fraction originating from the disk are listed in Table 3. After correction of disk contribution, the elemental concentrations of abrasion dusts were found to equal those of the bulk pads reported in our previous paper (*16*). Therefore, F_{disk} was precisely estimated, enabling the Sb emission factor from automobiles to be determined.

Sb Emission Factor from Automobiles. The dust emission could be regressed by the automotive braking parameters of the initial kinetic energy loading to the friction surface and the braking time (see Figure 4). Then, the emission factors of brake abrasion dusts were calculated using eq 2 in the several cases of typical braking conditions as shown in Table 4a. The estimated emission factors for the brake abrasion dusts and Sb are listed in Table 4b. The emission factor of abrasion dusts was estimated as the average value of 6.0 mg/braking/car. This emission factor corresponds to 5.8 mg/braking/car for PM_{10} (97%, the averaged mass fraction of PM_{10} for pad I was used.) and 3.9 mg/braking/car for $PM_{2.5}$ (65%, the averaged mass fraction of $PM_{2.5}$ for pad I was used.). We confirmed that the elemental composition was independent to the particle size of brake abrasion dusts in our previous work (*16*). Then, they were converted to Sb emission

factors by using the pad mass fraction (72%; the subtraction of the average disk mass fraction of 28% for pad I) and the Sb concentration in the abrasion dusts originating from pad I (0.78%; shown in Table 3). The Sb emission factors for the respective cases were determined as approximately 32 μg Sb/braking/car for PM_{10} and 22 μg Sb/braking/car for $PM_{2.5}$ (Table 4b).

Any discussion of the generality of these estimated emission factors should account for the uncertainties in the determination procedure. The major uncertainties should be the variation in emission amounts and Sb concentrations among the different varieties of pads I, II, and III. As shown in Table 2, a maximum of 43% of relative standard deviation was observed in dust emissions among the three different pads. Moreover, 41% of relative standard deviation was also observed in Sb concentration among the three different pads as shown in the Table 3. Therefore, the combined standard uncertainty of the Sb emission factor was evaluated as 59% with regard to these two major factors. Although there is some large uncertainty with the Sb emission factor, our data will be essential to the modeling of atmospheric Sb concentration alongside roadways and also to the evaluation of Sb source apportionment.

Acknowledgments

This research was supported in part by a Grant-in-Aid for Young Scientists (B), 19710022, 2007 from the Ministry of Education, Science, Sports, and Culture, Japan. We thank Hirokazu Kimura (Infectious Diseases Surveillance Center, National Institute of Infectious Diseases), Hiroshi Tago (Gunma Prefectural Water Quality Analysis Center), Kimiyo Kumagai (Gunma Prefectural Institute of Public Health and Environmental Sciences), Satoru Udagawa (Tokyo Dylec, Co.), Eiichi Yoshida, Takeo Aiba, Yasuo Takagi, and Yosuke Sasaki (Akebono Brake Industry, Co., Ltd.) for providing advice and technical assistance.

Literature Cited

(1) Schwartz, J.; Dockery, D. W.; Neas, L. M. Is daily mortality associated specifically with fine particles? *J. Air Waste Manag. Assoc.* **1996**, *46*, 927–939.

(2) Borja-Aburto, V. H.; Castillejos, M.; Gold, D. R.; Bierzwinski, S.; Loomis, D. Mortality and ambient fine particles in southwest Mexico City. *Environ. Health Perspect.* **1998**, *106*, 849–855.

(3) Dockery, D. W.; Pope, C. A.; Xu, X. An association between air pollution and mortality in six U.S. cities. *N. Engl. J. Med.* **1999**, *164*, 12–14.

(4) Calcabrini, A.; Meschini, S.; Marra, M.; Falzano, L.; Colone, M.; Berardis, B. D.; Paoletti, L.; Arancia, G.; Carla, F. Fine environmental particulate engenders alterations in human lung epithelial A549 cells. *Environ. Res.* **2004**, *95*, 82–91.

(5) Oberdoerster, G. Effects and fate of inhaled Ultrafine particles. *Am. Chem. Soc. Symp. Ser.* **2005**, *890*, 37–59.

(6) International Agency for Research on Cancer (IARC). Antimony trioxide and antimony trisulfide. In *Monographs on the Evaluation of Carcinogenic Risk to Human*; IARC, Eds.; World Health Organization: Lyon, 1989.

(7) Uexküll, V. O.; Skerfving, S.; Doyle, R.; Braungart, M. Antimony in brake pads—A carcinogenic component. *J. Clean Prod.* **2005**, *13*, 19–31.

(8) Weckwerth, G. Verification of traffic emitted aerosol components in the ambient air of Cologne (Germany). *Atmos. Environ.* **2001**, *35*, 5525–5536.

(9) Gao, Y.; Nelson, E. D.; Field, M. P.; Ding, Q.; Li, H.; Sherrell, R. M.; Gigliotti, C. L.; Van-Ry, D. A.; Glenn, T. R.; Eisenreich, S. J. Characterization of atmospheric trace elements on $PM_{2.5}$ particulate matter over the New York−New Jersey harbor estuary. *Atmos. Environ.* **2002**, *36*, 1077–1086.

(10) Furuta, N.; Iijima, A.; Kambe, A.; Sakai, K.; Sato, K. Concentrations, enrichment and predominant sources of Sb and other trace elements in size classified airborne particulate matter collected in Tokyo from 1995 to 2004. *J. Environ. Monit.* **2005**, *7*, 1155–1161.

(11) Gomez, D. R.; Smichowski, P.; Gine, M. F.; Sanchez-Bellato, A. C. Antimony: A traffic-related element in the atmosphere of Buenos Aires, Argentina. *J. Environ. Monit.* **2005**, *7*, 1162–1168.

(12) Krachler, M.; Zheng, J.; Koerner, R.; Zdanowicz, C.; Fisher, D.; Shotyk, W. Increasing atmospheric antimony contamination in the northern hemisphere: snow and ice evidence from Devon Island, Arctic Canada. *J. Environ. Monit.* **2005**, *7*, 1169–1176.

(13) Sternbeck, J.; Sjoedin, A.; Andreasson, K. Metal emissions from road traffic and the influence of resuspension: Results from two tunnel studies. *Atmos. Environ.* **2002**, *36*, 4735–4744.

(14) Pakkanen, T. A.; Kerminen, V. M.; Loukkola, K.; Hillamo, R. E.; Aarnio, P.; Koskentalo, T.; Maenhaut, W. Size distributions of mass and chemical components in street-level and rooftop PM_1 particles in Helsinki. *Atmos. Environ.* **2003**, *37*, 1673–1690.

(15) Lough, G. C.; Schauer, J. J.; Park, J.; Shafer, M. M.; Deminter, J. T.; Weinstein, J. P. Emissions of metals associated with motor vehicle roadways. *Environ. Sci. Technol.* **2005**, *39*, 826–836.

(16) Iijima, A.; Sato, K.; Yano, K.; Tago, H.; Kato, M.; Kimura, H.; Furuta, N. Particle size and composition distribution analysis of automotive brake abrasion dusts for the evaluation of antimony sources of airborne particulate matter. *Atmos. Environ.* **2007**, *41*, 4908–4919.

(17) U. S. Environmental Protection Agency (EPA). Mobile 6.1 Particulate Emission Factor Model Technical Description, (EPA420-R-03–001); EPA: Washington, DC, 2003.

(18) Japan Clean Air Program (JCAP). Technical Report for Atmospheric Dispersion Model (1), (PEC-2001JC-04); Japan Petroleum Energy Center: Tokyo, 2001.

(19) Kenny, L. C.; Liden, G. A technique for assessing size-selective dust samplers using the APS and polydisperse test aerosols. *J. Aerosol Sci.* **1991**, *22*, 91–100.

(20) Sioutas, C.; Abt, E.; Koutrakis, P.; Wolfson, J. M. Evaluation of the measurement performance of the scanning mobility particle sizer and aerodynamic particle sizer. *Aerosol. Sci. Technol.* **1999**, *30*, 84–92.

(21) Garg, B. D.; Cadle, S. H.; Mulawa, P. A.; Groblicki, P. J. Brake wear particulate matter emissions. *Environ. Sci. Technol.* **2000**, *34*, 4463–4469.

(22) Sanders, P. G.; Xu, N.; Dalka, T. M.; Maricq, M. M. Airborne brake wear debris: Size distributions, composition, and a comparison of dynamometer and vehicle tests. *Environ. Sci. Technol.* **2003**, *37*, 4060–4069.

(23) Talib, R. J.; Muchtar, A.; Azhari, C. H. Microstructural characteristics on the surface and subsurface of semimetallic automotive friction materials during braking process. *J. Mater. Process. Technol.* **2003**, *140*, 694–699.

ES702137G